Weak bond detection in composites using solitary waves

Taru Singhal

A dissertation
submitted in partial fulfillment of the
requirements for the degree of

Master of Science

in Aeronautics and Astronautics

University of Washington

2015

Reading Committee:

Professor Jinkyu Yang, Chair

Professor Ramulu Mamidala

Program Authorized to Offer Degree:
UW Aeronautics and Astronautics

University of Washington

Abstract

Weak bond detection in composites using solitary waves

Taru Singhal

Chair of the Supervisory Committee:
Assistant Professor Professor Jinkyu Yang
Aeronautics and Astronautics

A composite material is composed of fibers embedded in a matrix and is called Fiber Reinforced Plastic (FRP). Particularly, Carbon Fiber Reinforced Plastic (CFRP) has carbon fiber as the reinforcement. It has a high strength-to-weight ratio and is not less susceptible to fatigue or corrosion compared to metallic materials. Therefore, composite materials like CFRP find applications in aerospace industry due to their low weight and advanced mechanical properties. For large scale composite structures, smaller parts often need to be connected together. The connection of these parts could be done either by mechanical joints such as fasteners or by gluing them together using adhesives. This research focuses on bonded composite structures. A prevailing problem in bonded joints is the indeterminate nature of the strength of the adhesive bond. Low strength bonds, i.e., weak bonds, are very difficult to detect and may become the cause of catastrophic failure. Hence, this work aims to develop a technique based on highly nonlinear waves called solitary waves to detect weak bonds. Nonlinear solitary waves can be generated in a 1-D chain of granular crystals, which consists of discrete particles having nonlinear interactions. Solitary waves are high energy packets, which maintain a finite spatial width while traveling. These waves, traveling in the granular chain, can be transmitted into the specimen by making direct contact with the chain. The reflected wave pattern from the specimen can give information about the localized stiffness of the specimen. In this study, two kinds of CFRP specimens are fabricated -

one with pristine bond and the other with a weak bond. For making a weak bond specimen, mold release agent is used to coat the surface of CFRP laminate prior to bonding. This coating acts as an impurity at the bondline and is an example of poor surface preparation. First, standard tests such as the three point bending and the end notched flexure tests are conducted to demonstrate that the strength of the bond is reduced due to the presence of the release agent coating. Further, impact test by solitary wave injection is conducted to cause weak bonds to develop delamination and obtain the response of solitary waves reflected from the specimens. We study the reflected wave characteristics for weak bond detection. Two cases are considered; in the first case, two specimens - pristine and weak bond samples, both without having an initial crack - are tested. In the second case, two specimens - pristine and weak bond samples, both with an initial crack - are tested. The results differentiate the weak bond with the pristine bond based on reflected wave characteristics. This study shows promising results indicating the potential of solitary wave-based detection of weak bond for hot spot monitoring of composite-based structures.

TABLE OF CONTENTS

LIST OF FIGURES

LIST OF TABLES

ACKNOWLEDGMENTS

At the outset, I would like to express my sincere gratitude to the University of Washington to allow me to pursue this esteemed degree program at the Aeronautics and Astronautics department in the company of domain experts, giving me an opportunity to learn. First, I would like to thank my adviser Professor Jinkyu Yang, who provided me with the opportunity to work on this interesting problem prevalent in the aerospace industry. I am thankful to him for believing in me and trusting my abilities. I am grateful to Dr. Eunho Kim for his constant mentorship and support. His experience has been very instrumental in the success of this research. Further, I would like to thank Professor Anthony Waas in the Aeronautics and Astronautics department and Professor Ramulu Mamidala in the Mechanical Engineering department for their instruction and consultation on the subject matter. I would like to extend many thanks to Luke Richard whose guidance helped me carry out some of the key experiments during my research. Also, I would like to thank Michelle Hickner and Bill Kuykendall in the Mechanical Engineering department for allowing and guiding me to utilize the lab facilities to conduct my experiments. Finally, I would like to thank my parents and friends whose constant support enabled me to achieve my ambitions. I would like to acknowledge Toray Composites for providing material support.

Chapter 1

INTRODUCTION

1.1 Composite material

A composite, by definition, is a combination of more than one substance [1]. In engineering terms, a composite material is a material composed of fibers embedded in a matrix. The Carbon Fiber Reinforced Plastics (CFRP) have high strength in the direction of the fibers and they are not susceptible to fatigue or corrosion. Therefore, CFRP have been widely used in several applications. Composite structures, also referred to as 'composites', are structures made out of composite material. There are a variety of substances which can be used as fibers in a composite like glass, carbon fiber, kevlar, and boron. For matrix, there are epoxy, vinyl ester, and bismaleimide. The material that is used in this research is carbon fiber (T-800) embedded in an epoxy.

Composite materials find applications in a number of sectors from aerospace sector to sectors like automobiles, bio-medical devices, sports goods, etc. In recent years the scale of the composite material usage has increased manifold and also spread across a variety of applications, primarily due to its light weight and high strength properties. This also stresses upon the fact that the reliability of the structures made from composite materials need to be evaluated. Composite materials could fail in several modes like delamination, matrix cracking, joint failure, etc. This study focuses on one such factor - bonded joint failure due to weakness of the bond, which may cause catastrophic failure of the structure. Bonding of composites is a common practice to build large scale structures. But, the challenge is that a weak bond is not easy to detect and its failure is highly unpredictable. Hence, it is very important to characterize a weak bond using some measurable quantity which enables its detection.

1.2 Adhesive bond

An adhesive bond joins two or more structural components using a glue or adhesive. The adhesive is applied to the surfaces of each part and hence joined together. Adhesive bonding is becoming popular in the aerospace industry for composite structures. It is advantageous in many respects. Adams et.al. [2] mention the following advantages of using adhesive bonding over fasteners. Use of adhesives in a joint eliminates the need of mechanical fasteners which add weight to the structure and could cause stress concentration near the joint. The stresses around the adhesive bonded joint are uniform. Also the cost of mechanical fasteners can be higher than that of an adhesive. A uniform stress distribution is obtained when composites are adhesive bonded which ensures better life. Adhesive bonding can also act as a sealing. It is useful when there is a need to join dissimilar materials which may not be possible by welding or brazing. Smooth external surfaces inhibit fatigue crack propagation. Smooth surfaces can be obtained by using bonded joints. But there are certain limitations of adhesively bonded joints. Adhesive joints make disassembly and field repairs extremely difficult. Surface preparation is necessary before bonding the substrates. Adhesive bonds are susceptible to environmental degradation if not stored properly. The most important problem is the quality assurance of the strength of these bonds. The detection of a weak adhesive bond is crucial to maintain integrity of composite structures.

1.3 Weak bond

The force between adhesive and substrate is called adhesion and the force between the adhesive molecules itself is called cohesion. A bond becomes weak if either the adhesive or cohesive force is not enough. In that case, the adhesive is then not able to strongly bond the substrates. Figure 1.1(a) shows a debond and figure 1.1(b) shows a weak bond between two adherends. Debond is characterized by the absence of adhesive and separation of adherends. Weak bond does not create any separation between the adherends but is not strong enough to bond the adherends [3]. Marty et. al. [4] describe three conditions for

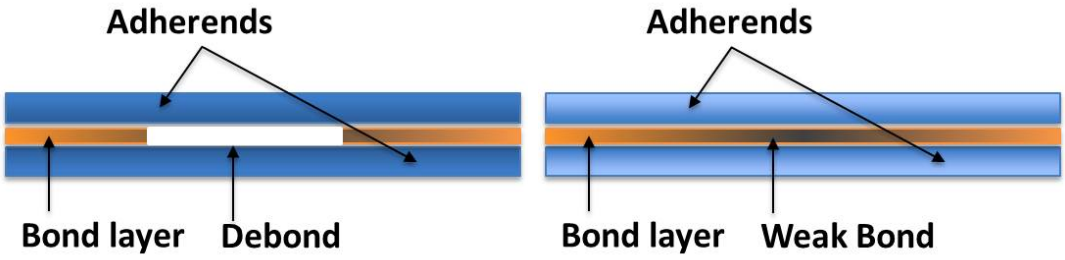

(a) Debond (b) Weak bond

Figure 1.1: Comparison of debond and weak bond

a bond to be characterized as a weak bond. These are (1) the strength of the weak bond must be below the nominal strength of the bond(2) bond failure mode must be adhesive, that is purely at the interface between the adherent and the adhesive (3) weak bond must be undetectable with classical amplitude C-scans. Weak bond may occur due to a variety of reasons. The presence of impurities in the adhesive or on the surface of the substrates is the most common reason. These impurities cause voids and defects and hinder proper bonding. These voids and defects are very small to be detected easily. In such cases, the stiffness of the bond remains the same but the strength reduces, sometimes significantly. Cohesive strength, however, may reduce due to the presence of moisture, inappropriate curing or poor adhesive material [5]. Due to the difficulty in strength measurement, it is challenging to determine if the bond is weak or strong. A weak bond is extremely difficult to detect and can cause catastrophic damage without prior warning. Hence, it is very important to devise a technique to determine the presence of weak bonds.

1.4 Literature review

Adhesives used for structural bonding of composite structures must possess adequate strength to transfer the loads through the joint. Adhesive bonding largely depends on the surface roughness as more is the surface roughness, more surface area is available for bonding.[6] For

a strong bond, the adhesive must wet the surface properly. Also, it must be ensured that the surface is clean and the adhesive is free from impurities. For an effective load transfer through the adhesive, the substrates are overlapped so that the adhesive is loaded in shear. Figure 1.2 shows different types of joint configurations. As shown in joint configurations in figure 1.2, adherends or the adhesive layer is often tapered as it aids the diffusion of loads through the structure. This minimizes the stress concentration and maximizes the joint strength [7]. Since physical testing of strength of the bonded composite structures can be expensive, the development of Non-Destructive Inspection (NDI) methods for composite structures may be less cost-intensive in terms of material usage. NDI methods focus on detection of defects prior to failure. Several methods have been developed over the years for ensuring the integrity of composite structures. Various NDI methods, developed for inspecting adhesive bonded joints in composite structures, were reviewed during this research. The principle of non-destructive testing essentially involves inspection of the specimen without causing any damage. The initial techniques were based on ultrasonic waves which were used to detect any defects by recording the reflected wave signal. But the ultrasonic methods have limitations when it comes to detection of weakly bonded joints. Brotherhood et. al. used ultrasound based methods to detect kissing bond [8]. Kissing bonds are defined as the one in which crack surfaces stay very close to each other. Holographic interferometry [9] was proposed as a potential method by Heslehurst. The interference of the reflected light produces an interference pattern over the 3-D image of the surface under investigation. Bossi et.al. [10] employed shock waves to induce motion in the free surface of the specimen. The plot of surface velocity profile was different for the weak bond as compared to that of a strong bond. Yang et.al. [11] worked on technique that involved study of modal parameters - frequency response and damping loss factor. The frequency response changed due to the change in joint stiffness. Hence, it was concluded that the presence of weak bond changed the stiffness which affected the frequency response. Digital Image Correlation [12] is yet another proposed method for the evaluation of the strength of the adhesive bond in composites. Further research is also being done to improve the current ultrasonic methods. These methods

would be discussed in detail in the following sections.

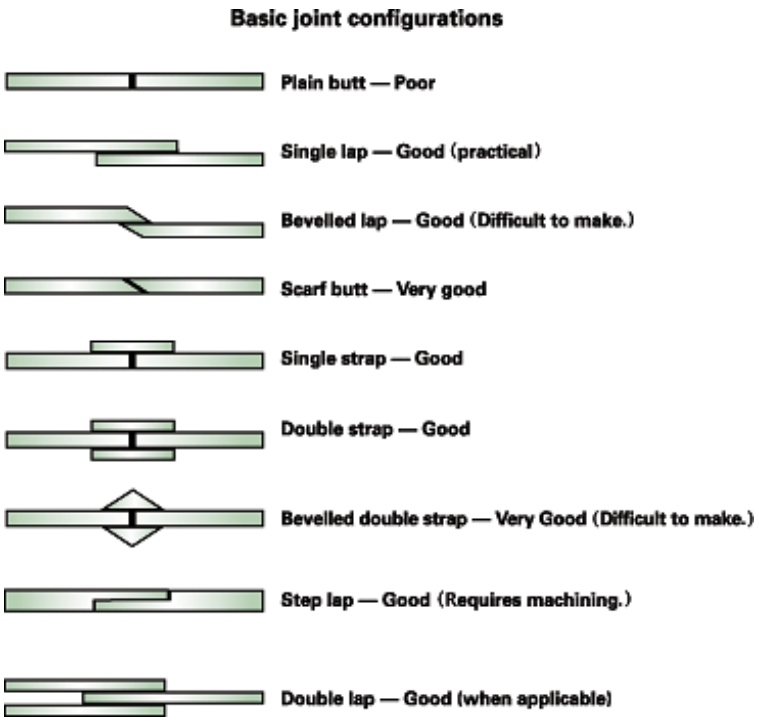

Figure 1.2: Various joint configurations [13]

Bond failure may occur due to the following causes; (a) complete voids, dis-bonds or porosity; (b) poor adhesion, i.e., a weak bond between the adhesive and the adherend; and (c) poor cohesive strength, i.e., a weak adhesive layer as shown in Figure 1.3. With advancement of time and technology, there has been a host of new techniques that have emerged, based on various principles that are employed for inspection of joint specimens. With every passing year, improvements are made in these techniques to achieve better results. Few such techniques are discussed below.

Kundu et.al. [14] used lamb waves to detect the kissing bonds. The principle behind this technique is that some Lamb modes may be more sensitive to interface defects than others. This is because high normal and shear stresses are generated at different depths of the specimen by lamb waves propagating under different modes. Although, it was shown

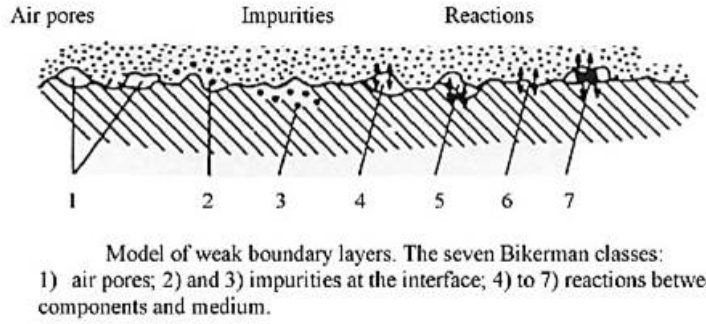

Figure 1.3: Weak boundary layer [9]

that most lamb modes were not sensitive to weak bonds except one specific mode. In 2001, Yang [11] and others used modal parameters to judge the strength of the bond. Specimens were prepared by varying the amounts of sanded or prepared surface since one of the causes of weak bond is poor surface preparation. Then, the frequency response and damping loss factors of these specimens were measured. To verify the results of modal tests, shear tests were also conducted and the results compared. Vibration frequencies, mode shapes and damping of a vibrating structure are referred as the modal parameters. These parameters depend on the stiffness and the mass of the structure. If there is a defect in the specimen, the local stiffness and mass is altered and hence the modal parameters then measured are different from those of a defect free structure.

In 2002, R. Bossi [15] proposed the use of laser based shock loads to load the adhesively bonded joint and hence monitor the free surface velocity using an interferometer. Energy deposition occurs when a shock wave is incident on a structure. Release waves are created at both the free surfaces and propagate into the structure, relieving the internal compressive stresses. The velocity of the free surface, which is in motion, is measured to determine the failure/survival of the joint. A surface velocity profile is plotted by the observations of the oscillation of the free surface using a laser interferometer. Initially, a low dose of shock is given to the specimen and the velocity profile is plotted. This works as the baseline plot. Further, a stronger shock wave is made to strike and free surface velocity profile is plotted.

Finally, a low dose is given and the velocity profile thus obtained is compared to the previous profile obtained.

Heslehurst proposed optical methods in 2009 [9]. The analysis of diffraction patterns of the light reflected from the surface of the bonded specimen helped detect debonding or weak bonds. Initially, a diffraction pattern is obtained with a strongly bonded specimen which serves as the baseline pattern. This pattern is then compared with the ones obtained from the weakly bonded specimen. For the weakly bonded specimen, the pattern changes due to local load transfer characteristic because of the local joint stiffness change. This change will enhance out of plane deformation which is detected by holographic interferometry.

In 2010, Ehrhart et. al. [16] studied various methods of quality assessment of adhesive bonded CFRP structures. The methods included ultrasonic techniques and laser based methods. The ultrasonic methods studied were - Normal incidence narrow-band pulsed spectrometry, Swept-frequency technique, Shear wave resonance ultrasonic technique and Oblique incidence ultrasonic technique. The laser based methods included - Laser Shock Adhesion Test (LASAT), Laser Bond Inspection (LBI) and Laser ultrasonic. These methods have been used for characterization of delamination and could potentially be used for weak bond detection. Laser shock adhesion test relies on disbonding a weak adhesive bond. The requirement for extensive experimental setup poses a limitation for these techniques.

More recently, in 2012, VijayaKumar, Bhat, and Murthy [12], proposed Digital Image Correlation (DIC) as a potential method of weak bond detection. Samples of adhesively bonded glass fiber reinforced plastic substrates were made with varying bond strengths. These samples were loaded till failure to determine the bond strength during which digital images were recorded and analyzed using the digital image correlation method. Patterns like lines, grids, dots or random arrays are used to analyze images. DIC is essentially high resolution image matching using algorithms that take the physics of the underlying deformation processes into account. In order to capture slightest deformations, dimensional changes of the order 10^{-5} m have to be resolved. The results were validated with the finite element analysis.

In 2013, Kumar et. al proposed evaluation of degradation in composite adhesive joints using ultrasonic method [17]. Samples used in the study were single lap shear joints of CFRP composites bonded with epoxy adhesive. Different amounts of polyvinyl chloride were used as the degradation causing agent. The joints were subjected to oblique incidence ultrasonic inspection and then subsequently subjected to mechanical loading in a testing machine till failure to determine its strength.

Ultrasonic techniques were one of the earlier methods developed for non-destructive inspection. Guided wave inspection [18] was proposed in 2013 as a technique of defect detection. Ultrasonic-based methods can be classified as bulk waves (small wavelength relative to dimensions of the material) or guided waves (wavelength larger than the smallest dimension of the material). Bulk wave methods are traditionally applicable for nondestructive evaluation. Guided wave methods are generally less sensitive to very small defects, but are advantageous (i) for structural health monitoring, (ii) when the bonded joint is inaccessible, and (iii) when kissing bonds are of concern. Tanary et.al [5] suggested non-destructive evaluation of bonded graphite/epoxy composites using acousto-ultrasonics. This technique consists of acousto-ultrasonic measurements followed by destructive shear tests were performed on single lap joint specimens made from graphite/epoxy adherends joined with FM 300 film adhesive.

Ehrhart et.al. [19], in 2014, demonstrated the use of laser shock adhesion for distinguishing bond strengths. It was observed that the laser shock method was able to differentiate the bonds by destructing the weak bond. The limitation of this method is that it can damage the CFRP during testing, which is undesirable.

Vijaykumar et.al [20] examined the suitability of techniques such as Ultrasonic through transmission method, Ultrasonic pulse echo method, Lamb wave inspection method, Real time digital X-ray radiography and On-line acoustic emission monitoring to evaluate bonded CFRP with varied bond quality. Results from ultrasonic through transmission method showed an encouraging trend.

1.5 Problem statement

The objective of this work is to understand the generation, propagation and mechanics of solitary waves as a potential weak bond detection method for Composite Fiber Reinforced Plastics (CFRP). It is aimed to also get a deeper insight in the behavior of CFRP, their manufacturing process and joining of composites. This research focuses on the detection of a weak bond using solitary waves. This would be accomplished by fabrication of weakly and strongly bonded specimens which are impacted by solitary wave. The reflected wave characteristics would be studied to gather information about the bond strength. The specimens would also be examined to check for any possible damage or delamination caused due to impact test.

This thesis is organized into three chapters following the chapter of introduction. The second chapter describes the theoretical aspects of the concepts like solitary wave, granular crystals and Hertzian contact. These concepts form the basis of the solitary wave impact test. Further, the third chapter focuses on the static tests done to demonstrate the successful fabrication and detection of weak bond in a CFRP specimen. The three point bending test and the end notched flexure test are described as the chosen static tests for this demonstration. The fourth chapter presents the details of the impact test using solitary wave. It consists of the impact test methodology and results for a pristine and a weak bond specimen. Discussion, conclusion and future scope are included in the fifth chapter.

Chapter 2

THEORETICAL BACKGROUND

2.1 Granular crystal chain

A granular crystal chain is a set of discrete spherical particles arranged consecutively in a line formation. Figure 2.1 shows a set of steel beads an example of granular media. When these spherical particles are compressed against each other, they deform at the point of contact. Nesterenko [21] discovered the generation of highly nonlinear elastic waves in one-dimensional granular media. These waves are called solitary waves. A solitary wave is generated when the striker bead of the same mass as the other beads in the chain impacts the first particle of the chain. However, when the striker bead is heavier than other beads, a train of solitary waves is induced [22].

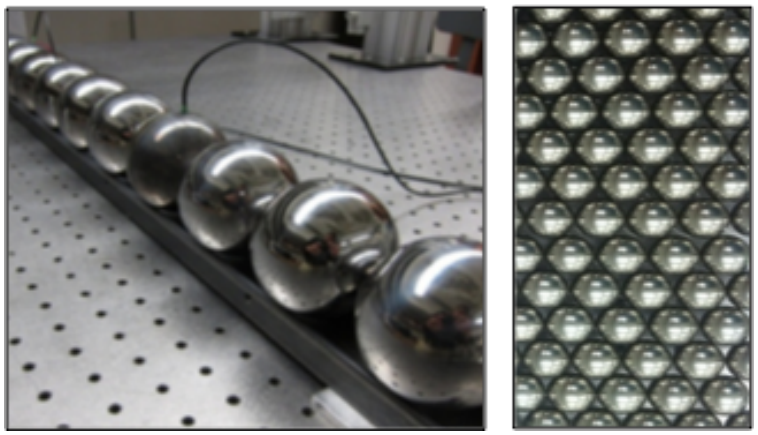

Figure 2.1: Granular crystals

The dynamic response of granular crystals is highly nonlinear i.e. the interaction between the grains is described by the Hertzian contact law. The compressive force - particle approach

(precompression) relation is nonlinear. Hertzian contact law is explained in the next section. When the precompression is absent in the granular chain or the grains in the chain merely touch each other without exerting any force on each other, there is complete nonlinearity in the system. Due to impact, the displacement of particles from their mean position is quite large as compared to the precompression, δ and therefore δ is neglected. Nesterenko [21] derived the exact solution to the differential equation describing this dynamic behavior as highly nonlinear solitary wave solution. In such a system, the oscillation of the particles about the mean position is absent and the particles tend to move uni-directionally. Nesterenko [23] characterized such systems as 'acoustic vacua' or no propagation of sound or acoustic wave. It was shown by Sen et. al. [23] that systems consisting of 1-D granular media support the generation and propagation of solitary waves. The solitary wave found in such discrete systems is supersonic and has a finite width which depends on the nature of the interface between the granular crystals. The spatial width is approximately five particle diameters. The key factors affecting the generation and dynamics of the solitary wave are the initial conditions and type of grain interface. The particle dimension and material can be changed to tune the propagation properties of the solitary wave.

2.2 Hertz's contact

When curved surfaces of elastic bodies are in contact with each other, ideally, it is a point contact. However when a force is applied to the two bodies such that they compress against each other, the contact no longer remains a point contact instead it is an area contact. Then, the contact mechanics is governed by the Hertzian contact law.

Hertz's Law for two spheres [24]: When there is compression between two identical spherical elastic particles, there exists a repulsive force which pushes them apart. This repulsive force between the two solid spheres increases as the compression increases. During the compression, there is an overlap, δ, between the two grains or particles. The repelling force is produced due to the elastic tendency of the grains which try to regain their original shape. Hertzian contact law is the solution of this linear elasticity problem for small deformations

and sufficiently stiff materials. Figure 2.2 shows a comparison of the relation between force and displacement described by linear Hooke's law and the nonlinear Hertzian contact law.

$$F = A\delta^{3/2}, A = \frac{E\sqrt{2R}}{3(1-\nu^2)} \tag{2.1}$$

where ν is the Poisson's ratio, R is the radius of the spherical body and E is the Young's modulus. The Poisson's ratio governs the expansion of the material in other directions during compression and the elastic modulus, E governs the stiffness of the material. Equation 2.1 suggests that the force experienced by the deformed particles is proportional to 1.5^{th} power of the approach or deformation, δ. The factor - 1.5 depends on the contact geometry between the grains. The more regular is the contact surface, the smaller is the index. In a dynamic system where the deformation, δ, is varying, but slowly enough that the material remains in equilibrium, the Hertz's law is still valid. As a quasi-static approximation, Antoine [25] states that the formula is valid as long as the speed of the waves in the chain is negligible compared to the speed of wave propagation (speed of sound) in the material of the beads. This assumption is important for our study which involves dynamically loading the specimen using a solitary wave.

Now, for our case, consider the 1-D chain of grains compressed against each other. The overlap at contact n between the particles n and $n-1$ is $\delta = (u_{n-1} - u_n)$ where u_n is the position of particle n. If $\delta > 0$, the force at the contact is given by equation 2.1. If there is no overlap or $\delta <= 0$, $F = 0$.

Applying the Newton's second law , the equation of motion for n^{th} spherical particle of mass m can be obtained and is given by equation 2.2 [26]

$$m\frac{d^2u_n}{dt^2} = A[(u_{n-1} - u_n)]^{3/2} - A[(u_n - u_{n+1})]^{3/2} \tag{2.2}$$

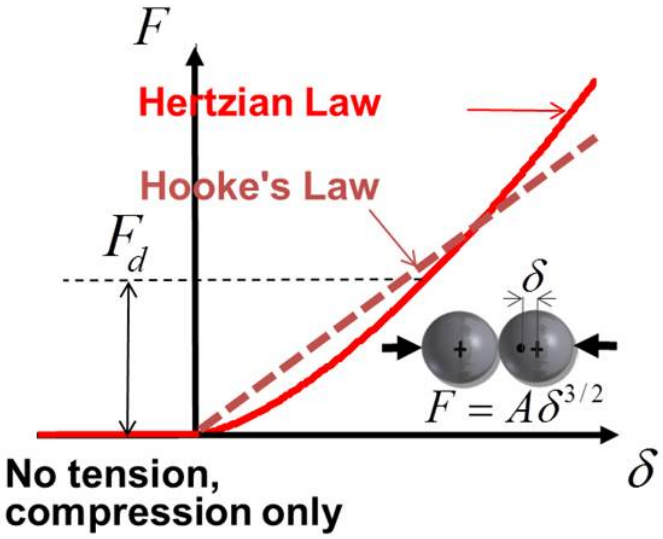

Figure 2.2: Hertz contact law

2.3 Solitary wave

A solitary wave is a highly nonlinear wave which has a finite spatial width [27]. Solitary wave formation can occur in discrete media such as 1-D granular chain. Localized nature of solitary waves arise due to balance between nonlinear behavior and the dispersive effects [28]. Solitary wave behaves like an energy bundle and maintains its shape when traveling at a constant speed as shown in figure 2.3. When it interacts with other solitary wave, it does not lose its structure and form except for a possible phase shift.

According to previous studies, the geometry, the mechanical properties, and the boundary conditions of an adjacent medium affect the reflected waveform of solitary wave [29]. In general, the potential energy of a wave defines its shape and energy content. The dynamics of a wave is governed by its potential as well as kinetic energy [24]. As the waves propagate, dispersion tends to occur and the amplitude of the wave attenuates. Traveling waves can be

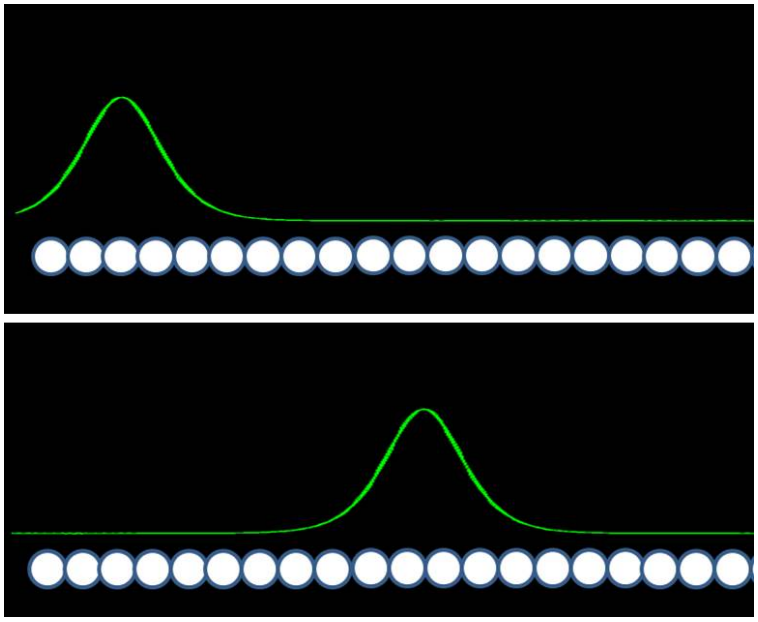

Figure 2.3: Solitary wave propagation through granular crystal chain

described by the Equation 2.3.

$$u(x,t) = Asin(kx - \omega t + \phi_0) \tag{2.3}$$

where A is the amplitude, k is the wave number, ω is the angular frequency and ϕ_0 is the phase. This is the solution of the linear differential equation of motion Equation 2.4.

$$\frac{\partial^2 u}{\partial t^2} = -\omega^2 u(x,t) \tag{2.4}$$

As mentioned earlier, a highly nonlinear solitary wave is generated when the grains in the 1-D chain barely touch each other and there is no precompression. However, when given a large static compression as compared to the amplitude of dynamic excitation, the systems can be described as a linear or weakly nonlinear wave medium. The weakly nonlinear soliton generated in this medium are described by the KdV equation. The simple form of Kortewegde Vries (KdV) equation is stated in Equation 2.5.

$$\frac{\partial u}{\partial t} = u\frac{\partial u}{\partial x} + \frac{\partial^3 u}{\partial x^3} \tag{2.5}$$

where $u(x,t)$ is the nondimensional velocity of a pulse traveling in a deep, long and narrow channel with a small wave amplitude. But, in the case of slightly precompressed or uncompressed chain, the dynamic behavior of the system is highly nonlinear. The precompression, δ, can be neglected as it is negligible compared to the particle displacement due to dynamic loading. The displacement of the neighboring particles can be expressed in terms of power series about the position n using the long-wavelength approximation [30].

$$u_{n-1} = u - u_x(2R) + 1/2u_{xx}(2R)^2 - 1/6u_{xxx}(2R)^3 + 1/24u_{xxxx}(2R)^4 + ... \tag{2.6}$$

$$u_{n+1} = u + u_x(2R) + 1/2u_{xx}(2R)^2 - 1/6u_{xxx}(2R)^3 + 1/24u_{xxxx}(2R)^4 + ... \tag{2.7}$$

Substituting equations 2.6 and 2.7into equation 2.2. The analytical expression obtained after simplification is given by:

$$u_{tt} = -c^2(-u_x)^{3/2} + \frac{a^2}{10}[(-u_x)^{1/4}((-u_x)^{5/4})_{xx}]_x \tag{2.8}$$

where u is the displacement, $a = 2R$ is the particle diameter, c^2 is given by $\frac{2E}{\pi\rho_0(1-\nu^2)}$ with c being a material constant and ρ_0 is the particle density. The strain, $\xi = -u_x$, and $\xi \equiv -u_x > 0$. Nesterenko [21] gives an exact solution to equation 2.8:

$$\xi = (\frac{5V_s^2}{4c^2})^2 \; cos^4(\frac{\sqrt{10}}{5a}(x - V_s t)) \tag{2.9}$$

where V_s is the velocity of the solitary wave traveling in the chain. This velocity can be expressed as a function of the ratio of static and dynamic force $f_r = F_d/F_0$,

$$V_s = 0.9314(\frac{4E^2F_0}{a^2\rho^3(1-\nu^2)^2})^{1/6} \; \frac{1}{(f_r^{2/3} - 1)} \; \{\frac{4}{15}[3 + 2f_r^{5/3} - 5f_r^{2/3}]\}^{1/2} \tag{2.10}$$

When there is no precompression, equation 2.10 becomes:

$$V_s = 0.6802(\frac{2E}{a\rho^{3/2}(1-\nu^2)^2})^{1/3}\ F_d^{1/6} \tag{2.11}$$

Therefore, the nonlinear and discrete nature of the granular chain support the generation and propagation of Highly Nonlinear Solitary Waves (HNSW). Equation 2.11 shows that a nonlinear relation exists between the solitary wave speed and the maximum dynamic contact force, F_d.

Chapter 3

STATIC TESTS

Before directly conducting the impact test which involves dynamically loading the specimen by solitary wave, tests using static loading were conducted to get an estimate of the behavior of the weak bond. It is a challenge to create a weak bond whose strength is characterized by a measurable parameter such as amount of impurity introduced. This is important for this study as it will help in the calibration of applied energy using solitary wave for a particular strength of the bond. To prepare a weak bond, silicone based mold release agent was used in this study. CSM [31] showed that contaminants other than silicone based contaminants may not induce weakness in bonds.Therefore, two flexure tests - three point bending and end notched flexure test were conducted on the pristine and the contaminated specimen in order to study the response of the two specimens with different bond characteristics.

Interlaminar stress is the stress that occurs between the laminae in the in-plane direction. It is also known as the transverse shear stress. Interlaminar stress can cause separation of the laminae or delamination if it exceeds the interlaminar strength, thereby reducing the strength of the component [6]. The Classical Laminate Theory (CLT) ignores the interlaminar shear stress components [32, 6]. However, an accurate prediction of failure can only be made if these stresses are appropriately calculated. Debonding also is effected by the shear stress between the adherend and the adhesive. Since the composites laminates are directional and anisotropic, there are various damage modes. These modes occur due to complex state of local stresses caused due by quasi-static and dynamic loads. During bending, transverse shear and normal stresses are induced in the laminate [33]. Low stiffness and strength in the through thickness direction enable these stresses to cause interlaminar delamination. Similar condition prevails between the laminate and the adhesive in case of bonded composites.

Hence, to evaluate the interlaminar shear stresses, three point bending test was chosen. Ealias et. al. [32] discuss an analytical approach to determine interlaminar shear stress of adhesive bonded structures using Finite Element Analysis (FEA). Ullah and others [34] used a simple FEA model to simulate multiple delaminations. This approach can be used to simulate bending of CFRP specimen and optimize parameters such as thickness and layup.

The three point bending test was conducted to demonstrate the variation in flexure strength, interlaminar strength as the strength of the adhesive bond changes in the CFRP specimen [35]. Similarly, end notched flexure test was conducted to determine the mode II fracture toughness or the critical stress intensity factor for the case of pristine bond and weak bond and observe the difference in fracture toughness values.

3.1 Three point bending test

The three point bending was conducted in accordance with the ASTM standard - D7264 [36] . The details of the test are described below. Figure 3.1 shows the schematic setup of the bending fixture with the specimen loaded on it. The three pins on the fixture hold the specimen. Two support pins at the bottom maintain simply supported boundary condition. The pin at the top and in the middle of the specimen is used to apply load at the center in the vertical direction. Figure 3.2 shows the top and the side view of the specimen with the specified dimensions. The specimen was fabricated using T800 prepreg lamina. After stacking the laminae according to the desired layup, here - $[0_3/90_3/0_3/Adhesive]_s$, the stack was placed in the hot press for curing. Once cured, the laminate was cut into the desired dimensions. Bonding surfaces are sanded with 150 grit sand paper. The adhesive - *Loctite EA* 9394, was prepared with a [100(epoxy):17(curing agent)] mixing ratio. For the pristine case, adhesive was applied to two pieces of laminate and the pieces were bonded together like a sandwich. After bonding the specimens, they were cured at 180 degrees F for 1 hour with a pressure 30 kPa. For the weak bond, before the application of adhesive, coating of silicone based mold release agent - *Evercoat* 5685, was applied as a film on the surface of the laminate. After the coating dried, adhesive was applied and cured in the similar manner as the pristine case.

In the figure 3.2, the grey rectangular area suggests the location of application of the release agent on the specimen. The specimen test matrix is shown in table 3.1. Three kinds of specimens were fabricated - specimens having 0 coating of release agent (control specimens), specimens having 2 coatings of release agent, and specimens having 6 coatings of release agent. 5 specimens of each kind were tested.

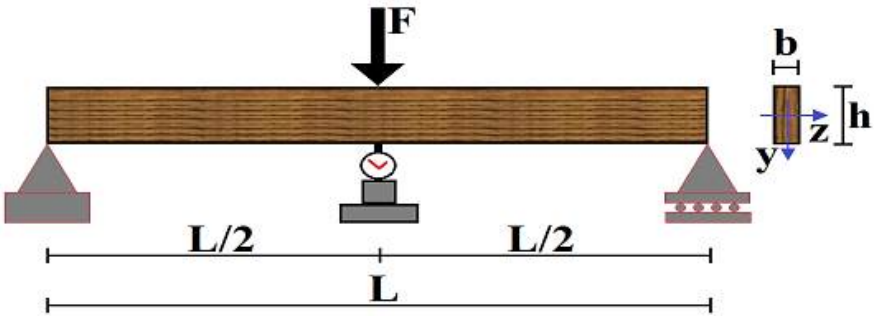

Figure 3.1: Three point bending test [37]

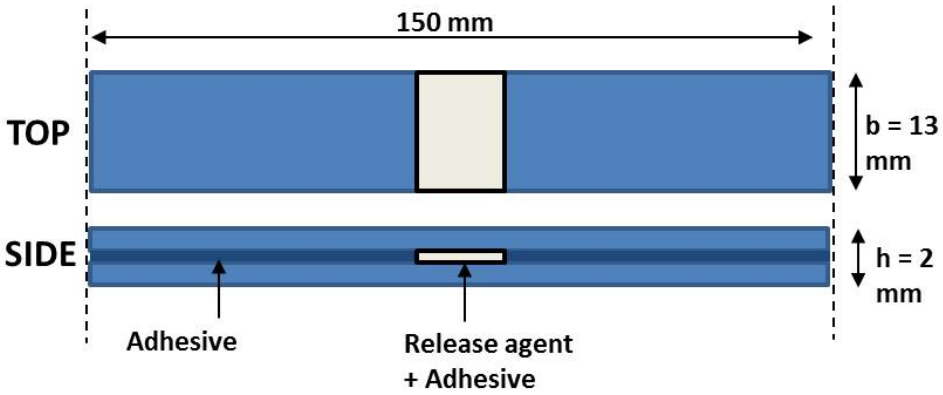

Figure 3.2: Specimen details for three point bending test

Specimen type (ID)	Surface treatment	Number of specimen
Control (0)	No release agent coating	5
Contaminated (R2)	Release agent coating 2 times	5
Contaminated (R6)	Release agent coating 6 times	5

Table 3.1: Experiment test matrix

3.1.1 Experiment details

The three point bending test was conducted using the Instron as shown in figure 3.3. The span of the support pins was 128 mm. It was ensured that the loading pin was exactly in the center of the support span. Load was applied at a rate of $1mm/min$. Load application continued until a loud cracking sound was heard. This signified delamination or damage to the specimen. The test was stopped at that point and the specimen was examined. The maximum load and displacement were recorded. This flexure test is commonly used to determine the bending strength of the material. During the bending test, the loading side is in compression and the other side (bottom) is in tension. The mid plane is in pure shear. Flexure strength and modulus were calculated using the EulerBernoulli beam theory since the specimen is symmetric about the central plane. Equation 3.1 gives the flexure strength.

$$\sigma = \frac{M\ y}{I} \tag{3.1}$$

The flexure modulus was estimated using equation 3.2

$$E = \frac{Fl^3}{48\ \delta\ I} \tag{3.2}$$

The Interlaminar Shear Stress (ILSS) is the maximum shear stress existing between layers of a laminated CFRP. It is resposible for causing delamination in CFRP due to in-plane shear. From mechanics of materials, the maximum shear stress occurs at the neutral plane. This

was verified by Ullah et.al. [34] using numerical simulations. Therefore, for the debonding problem, maximum interlaminar shear stress was calculated using the force-displacement data from the three point bending test. It was calculated by equation 3.3

$$ILSS = \frac{3\ F}{4\ b\ h} \tag{3.3}$$

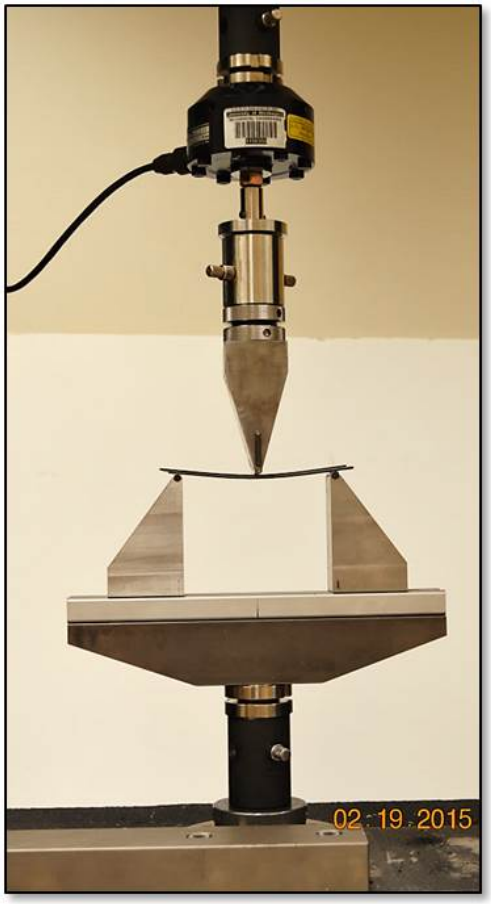

Figure 3.3: Loading machine by Instron used for three point bending test

Figure 3.4 shows one of the samples after the test. A crack appears within the plies causing delamination. Also, the adhesive layer cracks and the adhesive also debonds from the inner surface of the specimen where the release agent coating was applied to make the bond weak.

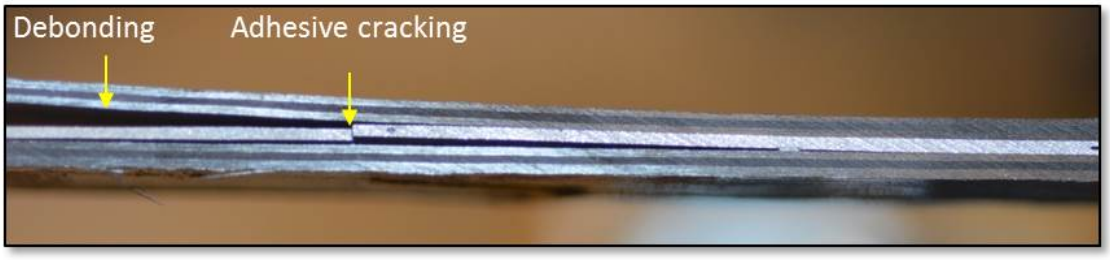

Figure 3.4: Specimen condition after bending test

3.1.2 Results

The specimen was inspected after conducting the test to gather information about the mode of failure and the bond state. The following observations were made:

- For the specimens with 0 coats of release agent:

The bending load damages the specimen instead of inducing delamination or debonding at the adhesive-composite interface.

- For the specimens with 2 and 6 coats of release agent:

The bending load causes the debonding in the specimens at the adhesive-composite interface. Further, the flexure strength, modulus and the interlaminar shear stress was calculated. Figure 3.5, 3.6(a) and 3.6(b) show the mean values of strength, modulus and interlaminar shear stress respectively with the respective maximum and minimum error as error bar.

The flexure strength and flexure modulus were calculated for the pristine and the weak bond specimens using the following analytical relations. From the results in table 3.2, it can be seen that a decreasing trend exists for the strength and modulus as the strength of the bond is decreased. Strength value for T800 composite from the Toray T800 datasheet is 1620 MPa and modulus is 150 GPa. Hence, the pristine bond specimen has the highest strength. A calibrated weak bond specimen was successfully fabricated.

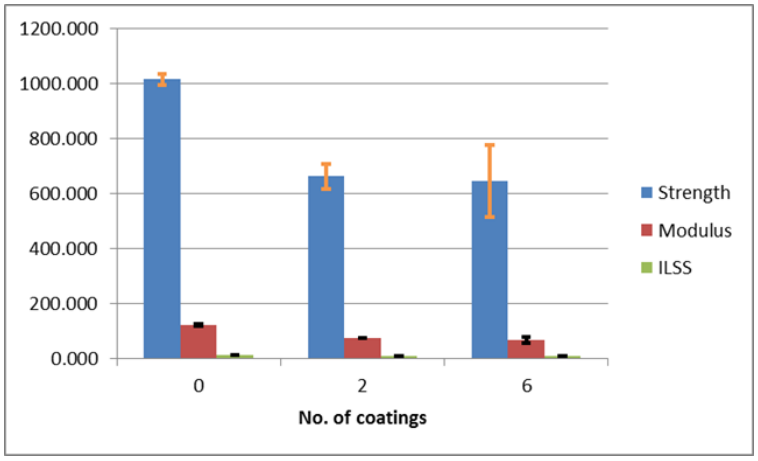

Figure 3.5: Measured flexure strength

RE Coating	0	2	6
Force (N)	805.00±15.1	525.50±36.6	512.00±103.6
Displacement (mm)	6.85±0.3	7.20±0.4	7.75±0.3
Flexure strength (MPa)	1013.77±19.0	661.79±46.2	644.79±130.5
Flexure modulus (GPa)	122.46±3.7	76.06±0.8	68.84±10.7
ILSS (MPa)	13.07±0.2	8.53±0.6	8.31±1.7

Table 3.2: Experimental results for three point bending test

3.2 End notched flexure test

Delamination in composites is essentially a fracture, which is basically separation of a part into pieces under the action of stress. Fracture can occur by applying load in three ways [38]. Mode I is the opening mode in which a tensile stress is applied normal to the plane of the crack. Mode II is the sliding mode, in which shear stress within the plane of crack, acting perpendicular to the crack front cause the fracture. The Mode III is also called the tearing mode. In this mode, out-of-plane shear stress acting parallel to the crack front cause the

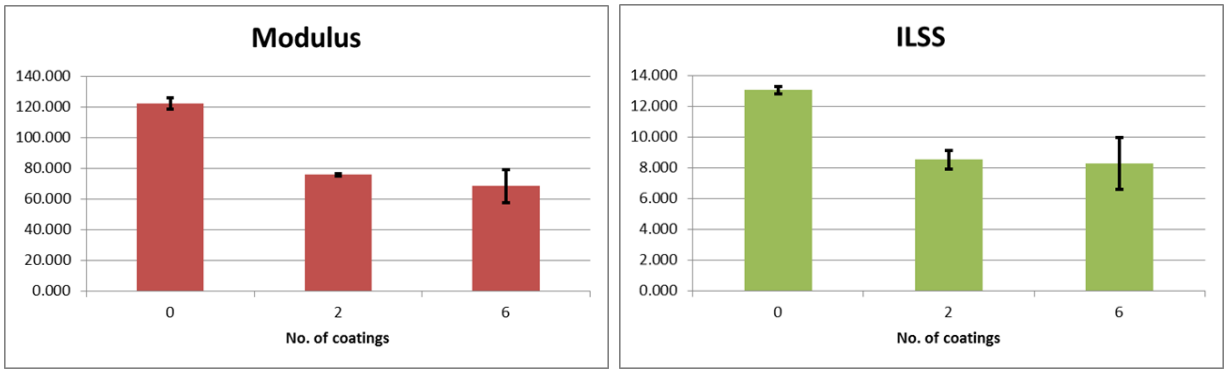

(a) Measured flexure modulus (b) Measured interlaminar shear strength

Figure 3.6: Three point bending test results

damage. Fracture toughness is the property which enables a material to resist fracture due to the presence of an initial crack. It is denoted by critical value of stress intensity factor which is the state of stress near the crack tip due to a remotely applied loading. The factors affecting the stress intensity magnitude are the geometry, size and location of the crack, and the load distribution on the specimen. Depending on the mode of crack propagation, the fracture toughness may be K_{Ic}, K_{IIc}, K_{IIIc}. Plain strain fracture toughness is given by equation 3.4. σ is the stress at which fracture occurs and a_c is the critical size of crack.

$$K_{IC} = 1.12\ \sigma\sqrt{\pi\ a_c} \tag{3.4}$$

$$G_{IIC} = \frac{K_{IIC}^2}{E} \tag{3.5}$$

The fracture toughness is related to the Strain Energy Release Rate (SERR) by equation 3.5. Strain energy release rate is the energy released during unit increase in crack or fracture area. If the strain energy release rate exceeds the critical value, fracture occurs. Szekrenyes [39] summarizes published experimental investigations conducted to determine the fracture properties of composite materials. The effects of fiber orientation, laminate and specimen configuration were discussed. In this study, loads act to support the fracture mode

II caused by in-plane shear stresses. To predict fracture, a measurable quantity such as the critical strain energy release rate was determined using the End Notched Flexure (ENF) test [33]. Prasad et.al. [40] review a variety of tests for determining the fracture toughness of composites. The different modes to evaluate the fracture energy and their suitability were discussed.

3.2.1 Experiment details

End Notched Flexure (ENF) test setup is similar to that of the three point bending test. However, the specimen used was different. The specimen was fabricated using 20 plies of T800 lamina with the layup - $[(0)_{10}]_s$. For the weak bond case, release agent was applied to the prepreg near the center. Once the coatings of the release agent dried, the stack of laminae was put in hot press for curing. In an ENF test, the specimen has an initial crack at one of the edges. The initial crack was introduced by inserting a piece of teflon tape at the middle from the top during layup and at one of the edges. Figure 3.7 shows the dimensions of the specimens used for the ENF test. The dimensions of the specimen were according to ASTM standard D7905 [41]. After curing, the laminate sustained a crack in the area where teflon tape was applied. The test matrix was the same as for the three point bending in table 3.1. All the specimen were painted with white spray paint along one of the long edges to monitor the crack growth. The test was conducted on the same Instron with the same fixture. Figure 3.8 shows the specimen loaded on the fixture of the bending machine. A static load at the rate of 1 mm/min was applied at the center of the specimen. In general, the positioning of the specimen on the test fixture is very critical and has to be according to the ASTM standard - D7905. The position of the cracktip with respect to the load application point governs the crack growth. So, to accurately determine the fracture toughness value, proper positioning is important. Before loading the specimen, the exact location of the support and the crack end was marked to record the crack initiation point. Then load was applied until the cracking sound was heard. The test was stopped and the specimen was observed for crack extension due to the load applied. The final location of cracktip was marked and the

crack extension was measured.

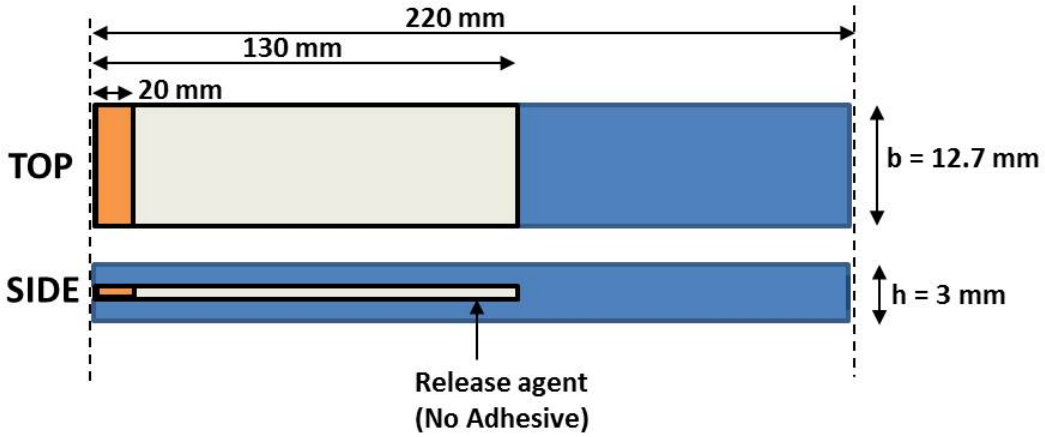

Figure 3.7: Specimen details for ENF test

As the specimen is loaded in bending, the crack tends to propagate. The amount of crack extension was measured along with the load applied to cause that extension. Using this information, the mode II fracture toughness (in plane) can be calculated.

3.2.2 Results

The specimen was observed after the test. The initial crack propagated along the mid plane. It was observed that the load required for crack propagation in case of weak bond was less than that required in case of a pristine specimen. The crack extended rapidly in case of a weak bond as compared to the pristine case.

The figure 3.9 shows the specimen with 2 coatings of release agent after ENF test. The markings show the position of cracktip after propagation. The specimen is split completely to show the inside surface. The slight color difference can be seen where the release agent was applied (weak bond area) compared to the rest of the specimen. The bottom picture in figure 3.9 below shows that the crack extended until the weak bond area quite easily and stopped as the weak bond region ends. This distinction indicates that release agent

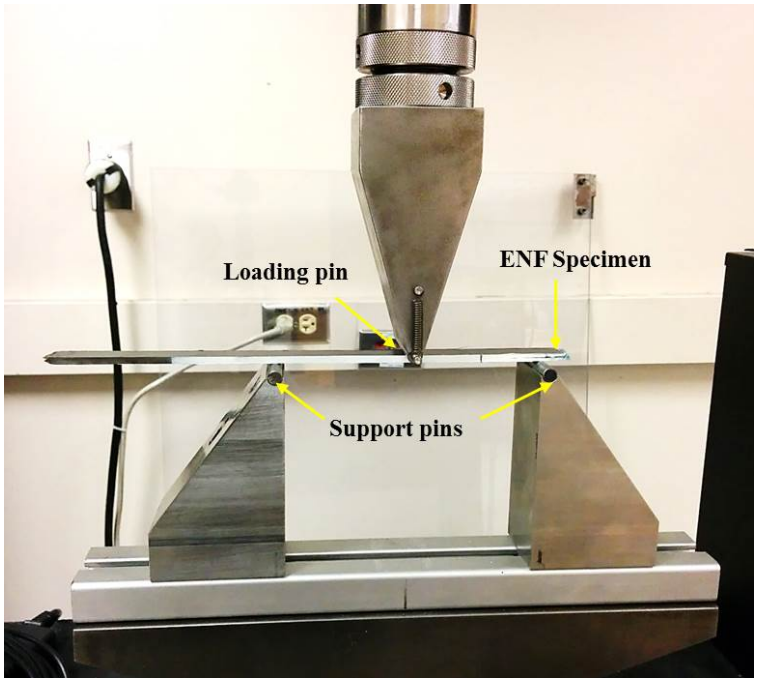

Figure 3.8: Experimental setup for ENF test

application makes the bonding weak between the plies. The strain energy release rate was calculated for each type of specimen using equation 3.6. Values obtained from literature [42] for CFRP are about $800 - 1200\ J/m^2$.

$$G_{IIC} = \frac{F^2}{2\ B}\frac{\partial C}{\partial a} \tag{3.6}$$

RE Coating	0	2	6
$G_{IIc}(J/m^2)$	795.19±109.4	710.43±34.6	265.38±46.7

Table 3.3: Experimental results for ENF test

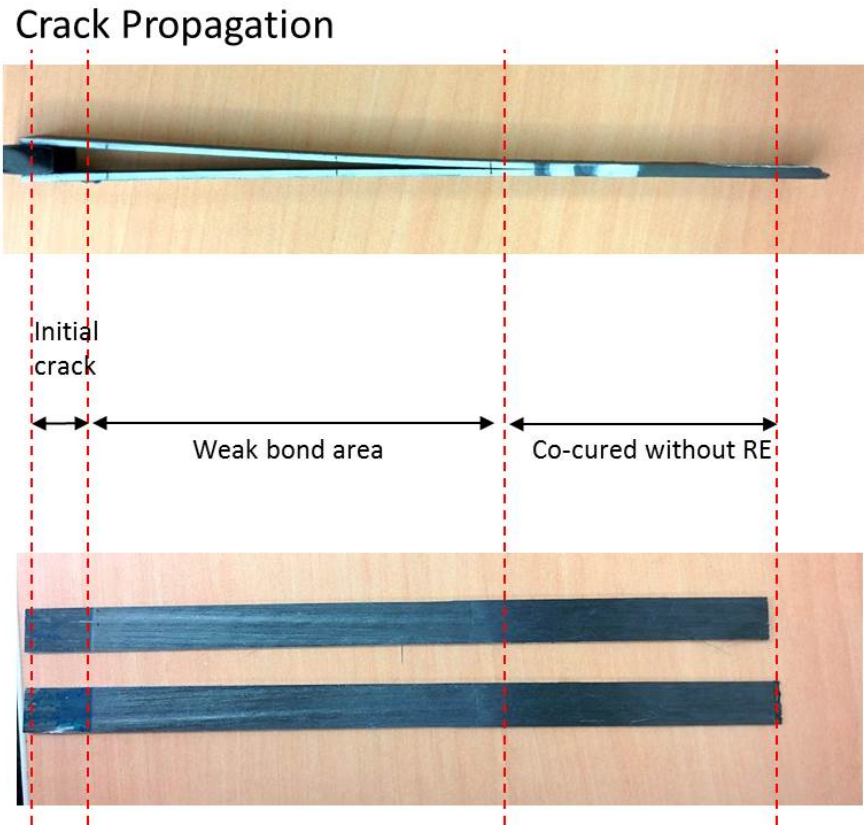

Figure 3.9: Specimen condition after ENF test

The decreasing trend of SERR was observed with increasing number of release agent coating or degree of weak bond. Figure 3.10(a) shows the strain energy release rates with errorbars for the three types of specimens. Figure 3.10(b) shows that the SERR for the specimen with 2 coatings is 11% less than that for the specimen with 0 coatings. Similarly, SERR for the specimen with 6 coatings is 67% less than that for the specimen with 0 coatings.

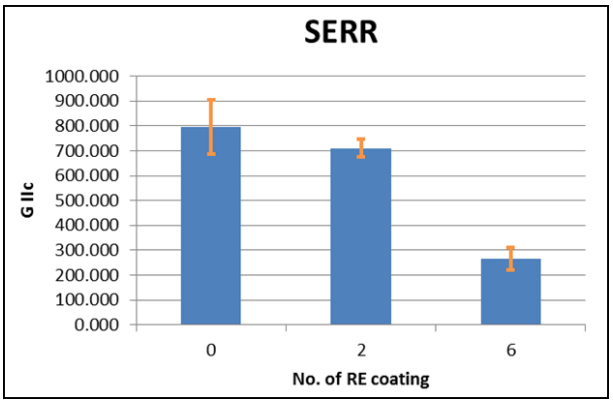

(a) Measured strain energy release rate

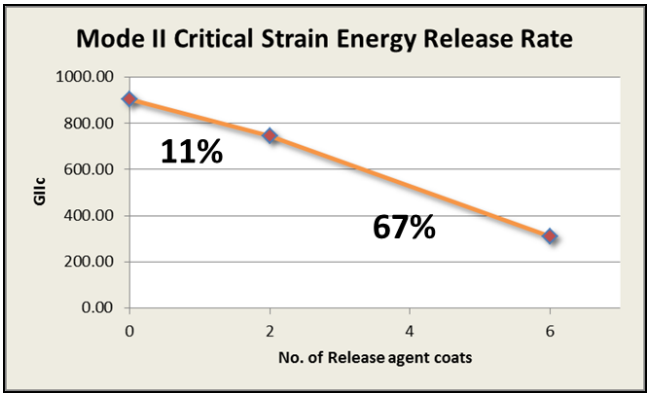

(b) Percentage reduction in SERR

Figure 3.10: ENF test results

Chapter 4

DYNAMIC TEST

4.1 Solitary wave impact test

4.1.1 Concept

As mentioned earlier in chapter 2, a solitary wave is generated by striking a granular crystal chain with a single striker grain. The impact energy and the presence of Hertzian contact between the crystals in the chain are responsible for the generation of a solitary wave. As shown in the figure 4.1 below, the solitary wave which is generated due to impact, travels through the chain and is incident on the specimen. This wave reflects back after striking the surface of the specimen [43]. The reflection pattern depends on the elasticity and geometry of the medium [44]. The incident and the reflected wave motion is captured by a sensor placed within one of the beads in the chain. The sensor bead holds a piezoelectric sensor at the center as shown in figure 4.2. One end of two connecting wires is soldered to the sensor and the other end is connected to the oscilloscope. The wave motion was studied to detect the presence of a weak bond.

4.2 Experiment details

The sample was fabricated from T800 prepreg laminae. The lay up consisted of 6 plies stacked as $[0/90/0]_s$. Before the plies were cured in hot press, the mold release agent coating was applied on the two layers at the center to get a weak bond. No coating was applied for the pristine bond case. Two kinds of specimens were fabricated - one without an edge crack and one with an edge crack, similar to the ENF test specimen as shown in figure 4.3. The beam specimen was fabricated similar to that for a three point bending test. The dimensions of the sample were 150mm $\times$ 15mm $\times$ 1mm. During the test, the support fixture span to

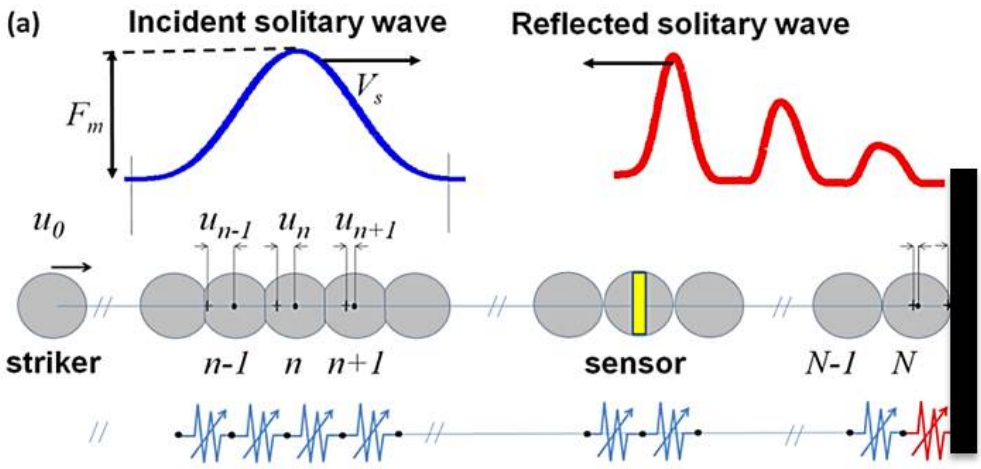

Figure 4.1: Concept of solitary wave impact test [43]

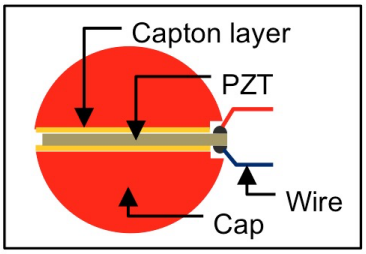

Figure 4.2: Sectional view of the sensor bead in granular chain [43]

specimen thickness ratio is maintained as 32:1 as suggested by ASTM standard for three point bending test [36].

Figure 4.4 shows the prepreg coated with mold release agent in the area around center. Another such ply is placed over it such that the coating is at the center in the thickness direction. The figure 4.5 below shows the side view of the ply stack. After making the plate by curing in the hot press, the plate is cut into strips using a diamond saw according to the dimensions required for the test. The figure 4.6 shows the test specimens cut using the wet saw and prepared with no coating and 6 coatings of release agent.

The figure 4.7 shows the experimental setup. It consisted of a chain of granular crystals

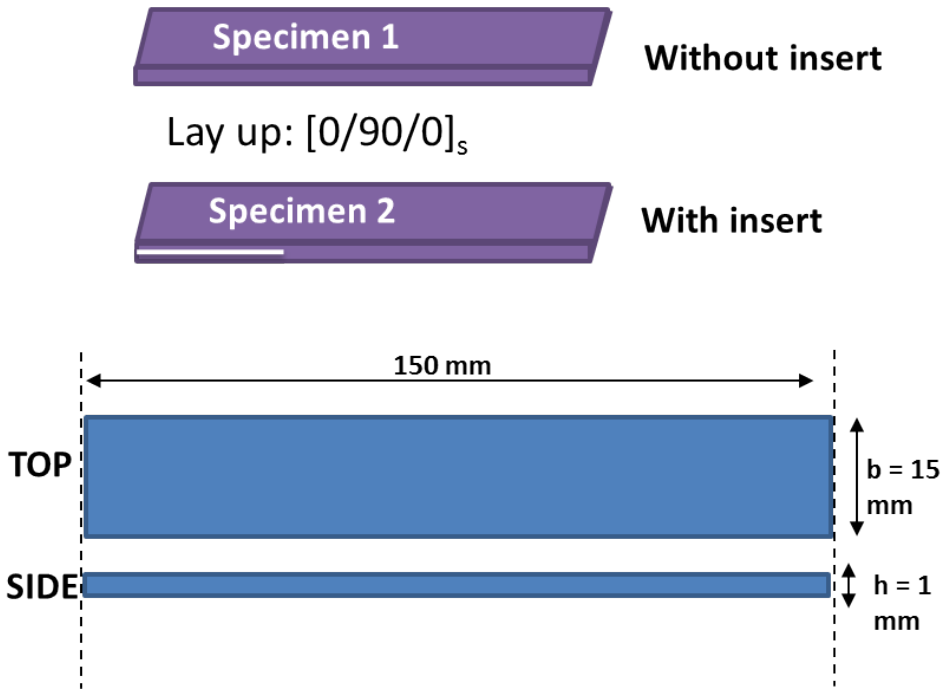

Figure 4.3: Specimen dimensions for impact test

i.e. chain of steel balls of 19.05 mm diameter and 28.1 grams, arranged vertically with the help of guiding rods of stainless steel. The striker bead was placed higher at a certain drop height. The bead with the piezoelectric sensor was placed at eighth place from the top in the chain. The sensor is usually placed somewhere in the middle of the chain to allow complete formation and travel of the wave as the width of the solitary wave is about five particle diameter [43]. The sensor was connected to the oscilloscope probes. The oscilloscope measured and displayed the incident and the reflected waveform of the solitary wave traveling through the chain. To get a clean and accurate waveform, it is important to keep the PZT sensor horizontal or perpendicular to the direction of wave propagation. The sensor bead rotated after the impact, so it was re-positioned before the next impact. The specimen was kept at the end of the chain at the bottom and was in contact with the last crystal as shown in figure 4.8. This enabled the impact of solitary wave onto the specimen. The specimen was

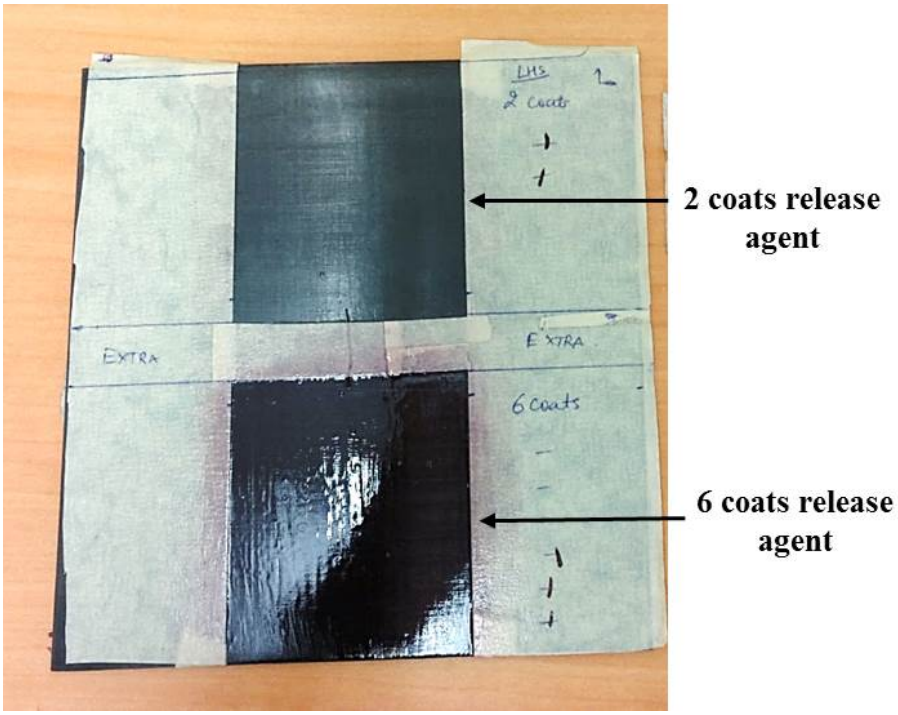

Figure 4.4: Release agent coating on specimen

simply supported to allow for bending. The impacted specimen was observed carefully to spot any visible damage or delamination. There was no damage found by the naked eye so to determine internal damage, C scan was done on the plate after each impact for both types of specimens. Overall, the process consisted of the following steps: impact the specimen with 50 cm drop height to induce crack propagation, impact the specimen with 10 cm drop height to obtain the reflected waveform, and conduct C-scan to check for damage. This process was repeated 5 times for each specimen.

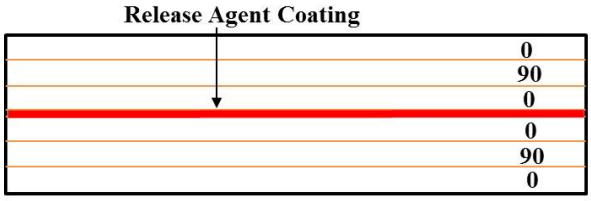

Figure 4.5: Ply layup for impact test specmen

Figure 4.6: Final impact test specimen

4.3 Results

First, the test was conducted on the specimens without a crack but for both pristine and weak bond case. The striker bead was dropped from a height of 10 cm. The reflected waveform for the pristine and the weak bond case was recorded and compared in terms of time of flight as shown in figure 4.9. Time of flight is defined as the time interval between the incident and the reflected wave. It was observed that the time of flight for the weak bond case was higher as compared to the pristine case as shown in figure 4.9. Also, there was no visible damage observed in either specimen - weak or pristine. Further, C scan was conducted to determine any internal delaminations. C scan is an imaging technique which is

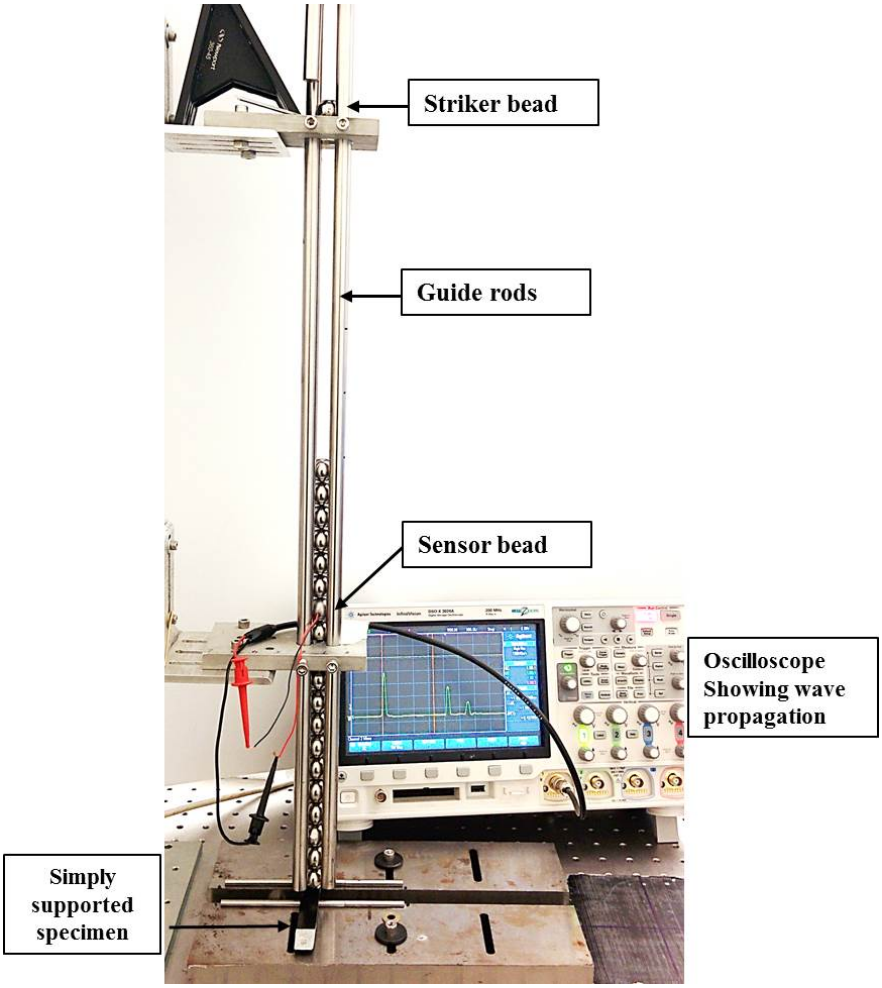

Figure 4.7: Experimental setup for impact test

based on ultrasound. Acoustic waves are incident on the specimen and reflected back from every surface they come across during propagation. Therefore, the first reflection is from the top surface, and the second reflection is from the back wall of the specimen. However, if there is a delamination present, the second reflection is from the delaminated surface and subsequent reflection from the back wall. Hence, this technique was used to determine any internal damage. There was no damage observed but a distinct spot in the C scan images was present at the point of impact. This shows that thickness changes slightly at the local

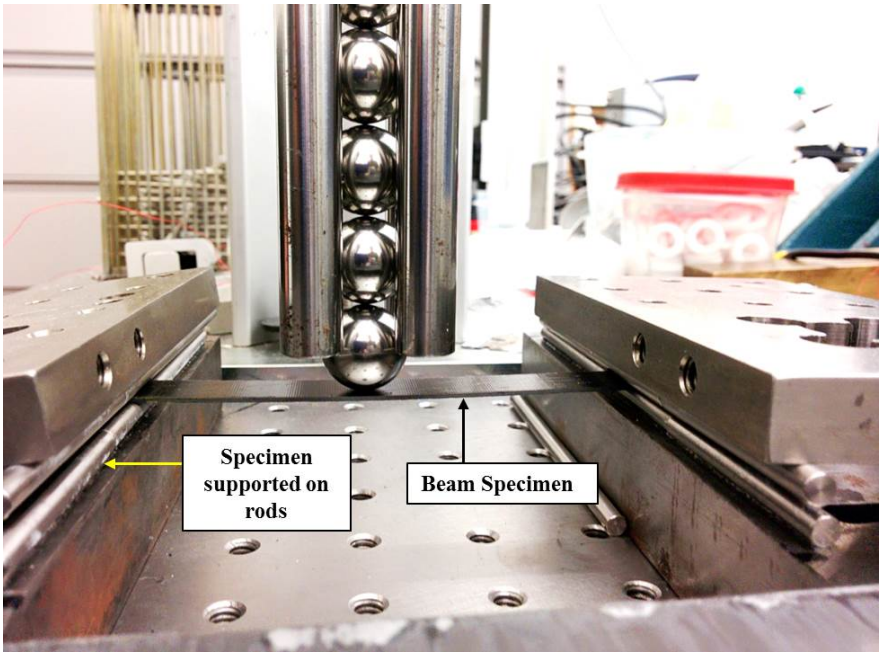

Figure 4.8: Specimen loaded under granular chain

spot.

In order to see the damage propagation due to solitary wave, another specimen - with an initial crack was used for the test. The specimens with 0 and 6 coating were tested one by one. This test comprised of two steps. In the first step, the specimen was impacted using a drop height of 50 cm. This was done to induce the propagation of crack which was present in the specimen. Sensor bead was removed from the chain during this step in order to avoid damage to the sensor. In the second step, the sensor was added to the chain and the striker was dropped from a height of 10 cm to obtain the waveform after the impact. Further a C scan was done each time to observe any progressive damage. The specimen position remained unchanged for the two steps but the specimen was shifted before the subsequent impacts according to the cracktip position. Further impacts upto 5 were made in a similar step-by-step manner and waveform was recorded for each impact.

Crack propagation was observed in weak bond case as opposed to the pristine case. The

wave response for both the cases is shown in figure 4.10(a). It can be seen that the time of flight in case of pristine case is lower which confirms the observation in the previous test. Also, due to the presence of crack, slight variation can be seen in the time of flight for each impact for the weak bond case as seen in figure 4.10(b). It is expected that the variation in the time of light may be due to the local stiffness change at the point of impact. This stiffness change may be due to the presence of the soft film of release agent present in the specimen.

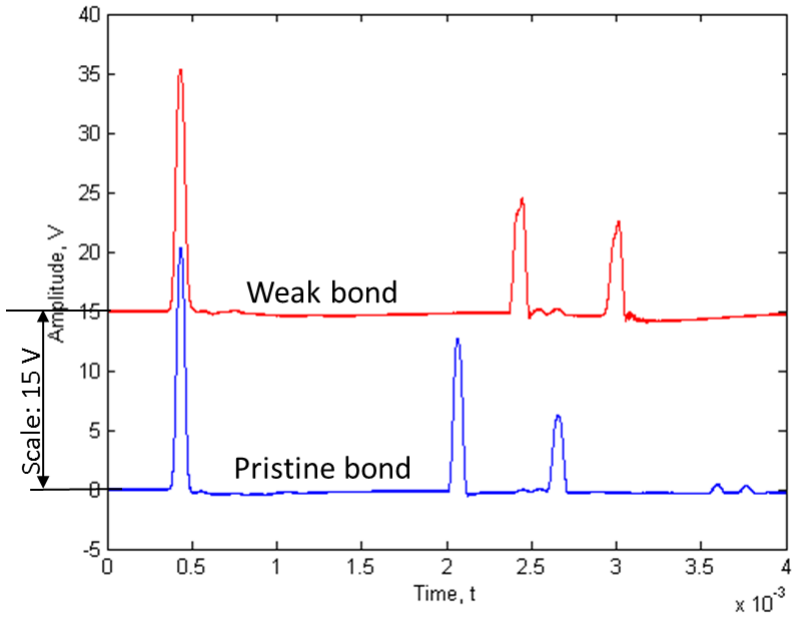

Figure 4.9: Waveform comparison before impact for pristine and weak bond

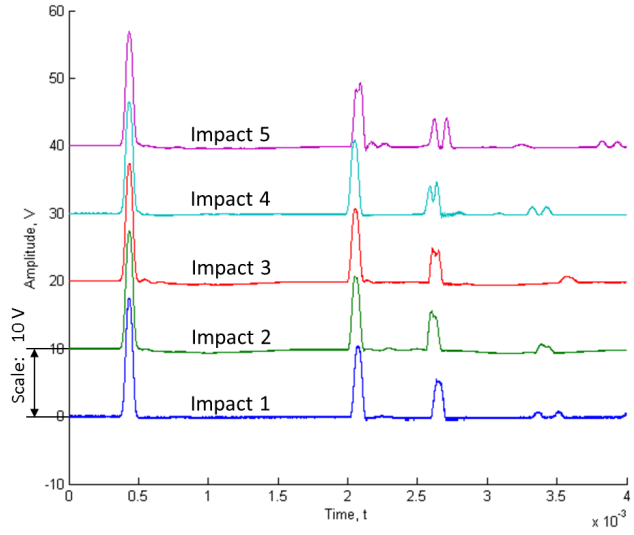

(a) Waveform for pristine bond specimen

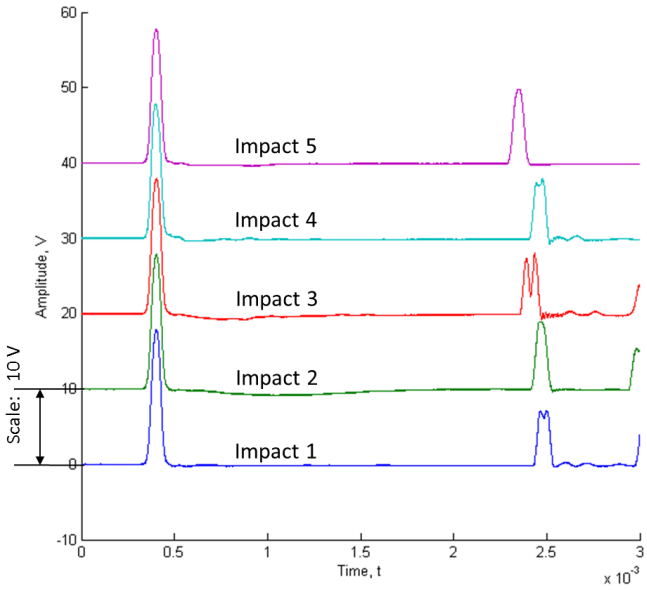

(b) Waveform for weak bond specimen

Figure 4.10: Waveform comparison after 5 impacts

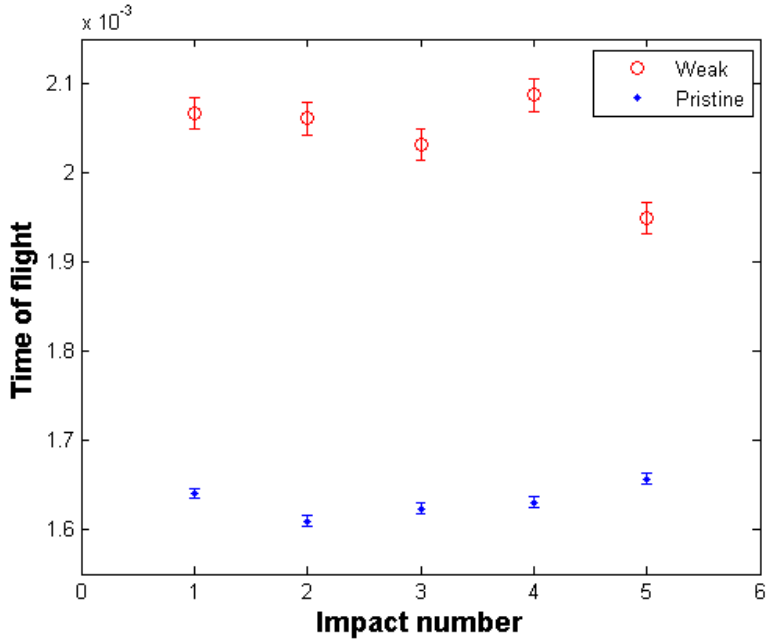

Figure 4.11: Comparison of time of flight for pristine and weak bond

The time of flight of the wave after each impact was compared for both the specimens in figure 4.11. The two important points that are evident in this figure are: (1) There is a higher time delay in case of weak bond (2) There is comparatively higher variation in time of flight in the case of weak bond. Clearly, the two kinds of bond can be distinguished on the basis of this data. Figure 4.12 shows the C scan images of specimen after each impact. The x and y axes shows the length and width scale of the specimen. The contour scale shows the time of flight scale. The blue area represents delamination or cracked portion of the specimen and the red are shows the pristine portion. Therefore, in the weak bond specimen, crack propagation can be noticed.

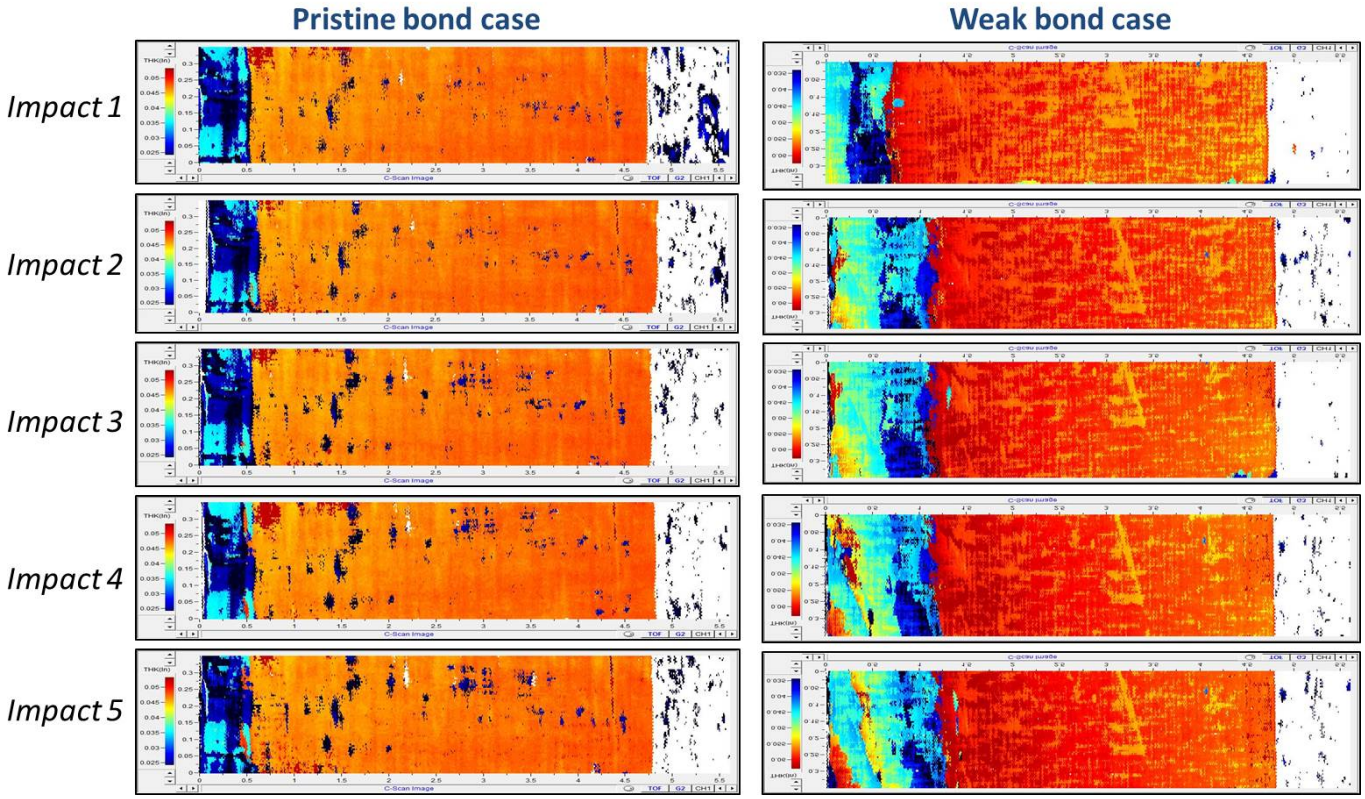

Figure 4.12: C-scan images of specimen after each impact

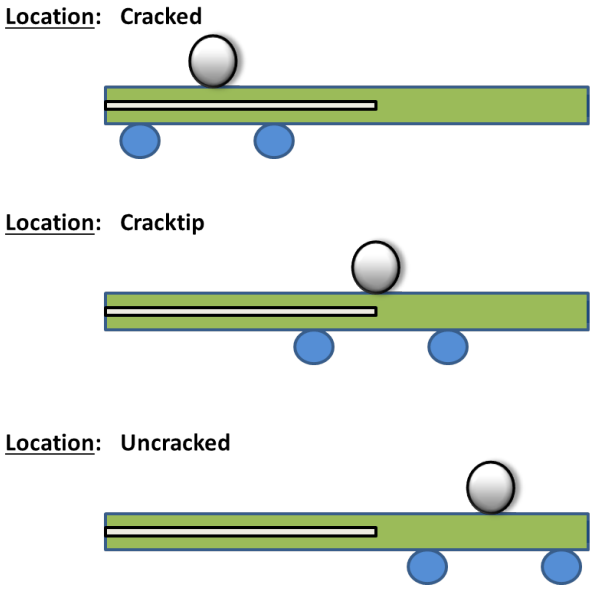

Figure 4.13: Locations for reflected wave response in a specimen with a crack

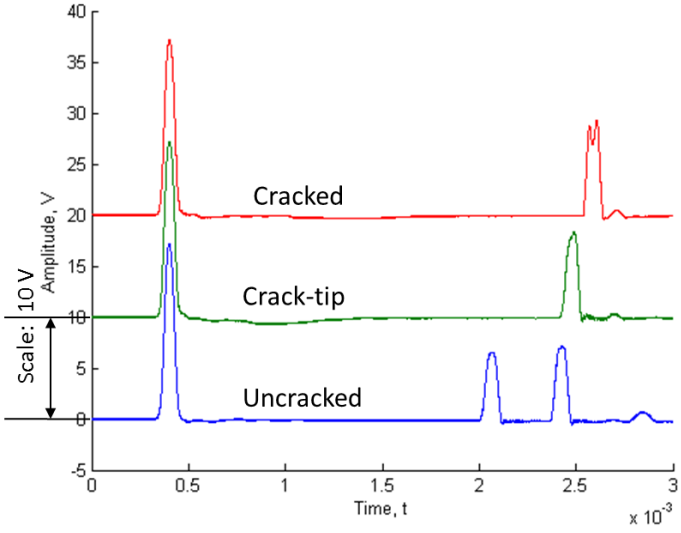

Figure 4.14: Comparison of reflected wave response at the selected locations of the specimen with a crack

Further, to determine the cause of variation in time of flight in the weak bond case, wave responses were obtained at three particular locations in the cracked specimen - the first location was where the specimen was cracked or a clear delamination, the second location was at the crack-tip and the third at the location where there was no crack. These locations are shown in figure 4.13. The results are shown in the figure 4.14.

The figure shows that the time of flight decreases in the order: cracked, crack-tip and uncracked location. As can be seen, the reflected wave for the cracked and the crack-tip locations occurs at very close time points, so slight change in the position of granular chain over the crack-tip may cause this variation.

Chapter 5

CONCLUSION

5.1 Discussion

Bonding of composites is becoming prevalent in the aerospace industry with the increase in the usage of composite materials for aircraft. In order to save weight, aircraft manufacturers consider replacing metallic parts with the composite materials. As a consequence, it is crucial to have composite parts integrated together using bonded joints. This study focuses on meeting one of the greatest challenges associated with bonded composites: detection of weak bonds. Occurrence of weak bonds in composites is a persistent problem. A weak bond can be detected by destructive testing. That is, we apply external excitation to break the weak bond, but not breaking a strong bonded part of the structure. Unfortunately, many non-destructive inspection techniques are not sensitive to the weak bond. This work is focused on solitary wave based detection of weak bonds via destructive approach. Solitary waves are highly nonlinear wave packets, which can be formed in 1-D granular media. The detection of weak bond using solitary waves takes two step approach. First, we create a delamination in the specimen using high-energy solitary waves. Then, we investigate the characteristics of the reflected solitary wave. Experimental work was done using pristine and weak bond specimens. The reflection pattern of solitary waves was studied to distinguish between strong and weak bond. Compared to other techniques, e.g., laser-based shock and ultrasound-based methods, this technique is advantageous in several ways. The biggest advantage is that the setup required to support solitary wave generation and propagation is compact and portable. Easy availability of components like steel beads, guide rods, and piezo-electric sensor make the setup inexpensive, yet reliable and accurate. Unlike laser-based techniques, no complicated power source is needed to excite the inspection medium;

excitation is achieved by a simple mechanical impact. This study shows promising results indicating the potential of solitary wave-based detection of weak bond for hot spot monitoring of composite-based structures.

5.2 Summary

In this study, the strength of a bond in bonded composites was investigated experimentally. Test specimens were fabricated using the lay-up - $[0/90/0]_s$ with 6 plies. Weak bond was realized by applying coatings of mold release agent to the bonding surface at the center of CFRP laminate prior to bonding. Different strengths of the bond were achieved by applying different number of coatings of mold release agent. Standard material tests - three point bending test and end notched flexure test were conducted to demonstrate the effect of impurity (mold release agent) on the strength properties of the specimens. A decreasing trend in the flexure strength, obtained from three point bending test, of the specimen was observed with increasing amount of mold release agent applied. Also, the rapid crack propagation was observed in the area of weak bond whereas crack propagation was not observed in the case of pristine bond. Two sets of specimens - pristine and weak, were tested using the solitary wave impact technique. The specimen was loaded under a vertically arranged chain of granular crystals (beads of stainless steel). A striker bead of the same size, mass and material was dropped over the first bead of the chain. The impact of the striker created a solitary wave which traveled through the chain and reached the specimen. The incident wave reflects back after striking the specimen. The reflected wave characteristics were recorded and studied. The observations in this study showed that the reflected wave characteristics like the time of flight vary for the different strengths of the bond in the specimens. Also, the reflected wave pattern varied when measured at cracked location, crack-tip location and uncracked location. The technique is sensitive to the presence of a crack or delamination.

5.3 Conclusion

The suitability of the proposed technique of solitary wave impact was examined for the detection of weak bonds. First, weak bond was successfully fabricated as demonstrated by the lower strength compared to the strength of the pristine bond specimen. The decrease in the fracture toughness with increase in weak bond degree was demonstrated using the end notched flexure test. Second, during the dynamic test using solitary wave, clear variation in the time of flight was observed for the pristine and the weak bond case. Also, delamination in the composite structure can be induced by high energy impact. High energy impact can be achieved by using large drop height which affects the impact velocity. However, for measurement purposes, very high energy is not required to get a clear incident and reflected waveform. Low velocity impact can be used to measure the bond strength. From the results, it can be concluded that solitary wave is very sensitive to the boundary conditions and presence of delamination. The solitary wave impact technique shows promising results in terms detecting a weak bond.

5.4 Future scope

Further study needs to be done by varying parameters like boundary conditions, thickness of specimen, bead size and drop height. The response of the specimen in terms of reflected wave characteristics is expected to be sensitive towards these parameters. Numerical simulations [45, 46] could be used to conduct the parametric study instead of carrying out experiments with all the combinations of these parameters. The amount of impact energy induced for weak bond detection can be optimized [47]. It is also important to determine the resolution of this technique i.e. detectable size of the weak bond using this technique. Additionally, weak bond creation using an impurity other than the release agent [48] could be considered and its effect on bond strength could be studied using solitary wave.

BIBLIOGRAPHY

[1] Isaac M Daniel, Ori Ishai, Issac M Daniel, and Ishai Daniel. *Engineering mechanics of composite materials*, volume 3. Oxford university press New York, 1994.

[2] RD Adams and PDRD Cawley. A review of defect types and nondestructive testing techniques for composites and bonded joints. *NDT international*, 21(4):208–222, 1988.

[3] Rikard Benton Heslehurst. Optical ndt of adhesively bonded joints. *Materials evaluation*, 67(7):837–842, 2009.

[4] Pierre Noël Marty, N Desai, and J Andersson. Ndt of kissing bond in aeronautical structures. In *Proceedings of the 16th world conference on NDT, Montreal*, 2004.

[5] S Tanary, YM Haddad, A Fahr, and S Lee. Nondestructive evaluation of adhesively bonded joints in graphite/epoxy composites using acousto-ultrasonics. *Journal of pressure vessel technology*, 114(3):344–352, 1992.

[6] Ronald F Gibson. *Principles of composite material mechanics*. CRC press, 2011.

[7] Robert D Adams, John Comyn, and William Charles Wake. *Structural adhesive joints in engineering*. Springer Science & Business Media, 1997.

[8] CJ Brotherhood, BW Drinkwater, and S Dixon. The detectability of kissing bonds in adhesive joints using ultrasonic techniques. *Ultrasonics*, 41(7):521–529, 2003.

[9] RB Heslehurst. Observations in the structural response of adhesive bondline defects. *International journal of adhesion and adhesives*, 19(2):133–154, 1999.

[10] Richard Bossi, Kevin Housen, Craig Walters, and Boeing Phantom Works. Laser bond inspection device for composites: Has the holy grail been found. *NTIAC Newsletter*, 30(2), 2005.

[11] Shuo Yang, Lan Gu, and Ronald F Gibson. Nondestructive detection of weak joints in adhesively bonded composite structures. *Composite Structures*, 51(1):63–71, 2001.

[12] RL Vijaya Kumar, MR Bhat, and CRL Murthy. Evaluation of kissing bond in composite adhesive lap joints using digital image correlation: Preliminary studies. *International Journal of Adhesion and Adhesives*, 42:60–68, 2013.

[13] URL:. www.designworldonline.com/7-steps-to-a-better-bond-line, .

[14] T Kundu, A Maji, T Ghosh, and Kl Maslov. Detection of kissing bonds by lamb waves. *Ultrasonics*, 35(8):573–580, 1998.

[15] Richard Bossi, Kevin Housen, and William Shepherd. Using shock loads to measure bonded joint strength. *Materials evaluation*, 60(11):1333–1338, 2002.

[16] Bastien Ehrhart, Bernd Valeske, Charles-Edouard Muller, and Clemens Bockenheimer. Methods for the quality assessment of adhesive bonded cfrp structures-a resumé. In *2nd International Symposium on NDT in, Aerospace*, 2010.

[17] RL Vijaya Kumar, MR Bhat, and CRL Murthy. Some studies on evaluation of degradation in composite adhesive joints using ultrasonic techniques. *Ultrasonics*, 53(6):1150–1162, 2013.

[18] Baiyang Ren and Cliff J Lissenden. Ultrasonic guided wave inspection of adhesive bonds between composite laminates. *International Journal of Adhesion and Adhesives*, 45:59–68, 2013.

[19] Bastien Ehrhart, Romain Ecault, Fabienne Touchard, Michel Boustie, Laurent Berthe, Clemens Bockenheimer, and Bernd Valeske. Development of a laser shock adhesion test for the assessment of weak adhesive bonded cfrp structures. *International Journal of Adhesion and Adhesives*, 52:57–65, 2014.

[20] RL Vijayakumar, MR Bhat, CRL Murthy, Donald O Thompson, and Dale E Chimenti. Non destructive evaluation of adhesively bonded carbon fiber reinforced composite lap joints with varied bond quality. In *AIP Conference Proceedings-American Institute of Physics*, volume 1430, page 1276, 2012.

[21] VF Nesterenko. Propagation of nonlinear compression pulses in granular media. *Journal of Applied Mechanics and Technical Physics*, 24(5):733–743, 1983.

[22] Stéphane Job, Francisco Melo, Adam Sokolow, and Surajit Sen. Solitary wave trains in granular chains: experiments, theory and simulations. *Granular Matter*, 10(1):13–20, 2007.

[23] Surajit Sen, Marian Manciu, Robert S Sinkovits, and Alan J Hurd. Nonlinear acoustics in granular assemblies. *Granular Matter*, 3(1-2):33–39, 2001.

[24] Surajit Sen, Jongbae Hong, Jonghun Bang, Edgar Avalos, and Robert Doney. Solitary waves in the granular chain. *Physics Reports*, 462(2):21–66, 2008.

[25] Antoine Levitt. Nonlinear waves in granular crystals. Master's thesis, University of Oxford, 2010.

[26] Stéphane Job, Francisco Melo, Francisco Santibanez, and Franco Tapia. Nonlinear waves in hertzian granular chains: Effects of inertial and stiffness heterogeneities. In *Proceedings of the International Congress on Ultrasonics, Vienna*, 2007.

[27] X Ni and P Rizzo. Highly nonlinear solitary waves for the inspection of adhesive joints. *Experimental mechanics*, 52(9):1493–1501, 2012.

[28] Jinkyu Yang, Claudio Silvestro, Sophia N Sangiorgio, Sean L Borkowski, Edward Ebramzadeh, Luigi De Nardo, and Chiara Daraio. Nondestructive evaluation of orthopaedic implant stability in tha using highly nonlinear solitary waves. *Smart Materials and Structures*, 21(1):012002, 2012.

[29] Stéphane Job, Francisco Melo, Adam Sokolow, and Surajit Sen. How hertzian solitary waves interact with boundaries in a 1d granular medium. *Physical review letters*, 94(17):178002, 2005.

[30] Devvrath Khatri. *Non-Destructive Evaluation of Material System Using Highly Nonlinear Acoustic Waves*. PhD thesis, California Institute of Technology, 2011.

[31] . *Internal report issued in 2002 by the Surface Treatment Department at CSM Materialtekink AB.*, 2014.

[32] Jeevan Ealias and Jenny John Mattam Lalmoni. Study of inter-laminar shear stress of composite structures.

[33] Alan A Baker Baker and Donald W Kelly. *Composite materials for aircraft structures*. AIAA, 2004.

[34] Himayat Ullah, Andy R Harland, Tim Lucas, Dan Price, and Vadim V Silberschmidt. Finite-element modelling of bending of cfrp laminates: Multiple delaminations. *Computational Materials Science*, 52(1):147–156, 2012.

[35] A Azzam and W Li. An experimental investigation on the three-point bending behavior of composite laminate. In *IOP Conference Series: Materials Science and Engineering*, volume 62, page 012016. IOP Publishing, 2014.

[36] . *ASTM D7264/D7264M-15, Standard Test Method for Flexural Properties of Polymer Matrix Composite Materials1 Composites*, 2014.

[37] André Luis Christoforo, Francisco Antonio Rocco Lahr, Elen Aparecida Martines Morales, Túlio Hallak Panzera, and Paulo Henrique Ribeiro Borges. Numerical evaluation of longitudinal modulus of elasticity of eucalyptus grandis timber beams. *International Journal of Agriculture and Forestry*, 2(4):166–170, 2012.

[38] Ted L Anderson and TL Anderson. *Fracture mechanics: fundamentals and applications*. CRC press, 2005.

[39] András SZEKRÉNYES. Overview on the experimental investigations of the fracture toughness in composite materials. *Hungarian Electronic Journal of Sciences, http://hej. sze. hu/, Mechanical Engineering Section, MET-020507-A*, 2002.

[40] MS Sham Prasad, CS Venkatesha, T Jayaraju, et al. Experimental methods of determining fracture toughness of fiber reinforced polymer composites under various loading conditions. *Journal of Minerals and Materials Characterization and Engineering*, 10(13):1263, 2011.

[41] . *ASTM D7905 / D7905M-14, Standard Test Method for Determination of the Mode two Interlaminar Fracture Toughness of Unidirectional Fiber-Reinforced Polymer Matrix Composites*, 2014.

[42] Hossein Saidpour, Mehdi Barikani, and Mutlu Sezen. Mode-ii interlaminar fracture toughness of carbon/epoxy laminates. *Iranian Polymer Journal*, 12(5):389–400, 2003.

[43] Jinkyu Yang, Devvrath Khatri, Paul Anzel, and Chiara Daraio. Interaction of highly nonlinear solitary waves with thin plates. *International Journal of Solids and Structures*, 49(13):1463–1471, 2012.

[44] Jinkyu Yang, Claudio Silvestro, Devvrath Khatri, Luigi De Nardo, and Chiara Daraio. Interaction of highly nonlinear solitary waves with linear elastic media. *Physical Review E*, 83(4):046606, 2011.

[45] Vipul Ranatunga. Finite element modeling of delamination crack propagation in laminated composites. In *Proceedings of the World Congress on Engineering 2011 Vol III WCE 2011*, 2011.

[46] Albert Turon Travesa et al. *Simulation of delamination in composites under quasi-static and fatigue loading using cohesive zone models*. Universitat de Girona, 2006.

[47] Eun-Ho Kim. *Composite damage model based on continuum damage mechanics and low velocity impact analysis of composite plates*. PhD thesis, KAIST, 2012.

[48] Dennis Roach, Kirk Rackow, and Randy Duvall. Innovative use of adhesive interface characteristics to nondestructively quantify the strength of bonded joints. In *Proceedings of the 10th European conference on non-destructive testing, Moscow*, 2010.